Kinetic lattice-gas model approach to collective diffusion in an ordered adsorbate in two dimensions

Magdalena A. Załuska-Kotur*
Institute of Physics, Polish Academy of Sciences, Aleja Lotników 32/46, 02-668 Warsaw, Poland

Zbigniew W. Gortel†
Department of Physics, University of Alberta, Edmonton, Alberta, Canada T6G 2J1
(Received 5 April 2005; revised manuscript received 24 October 2005; published 27 December 2005)

A recently developed approach to microscopic kinetics of an interacting lattice gas is applied to derive an algebraic expression for the coverage dependence of the collective diffusion coefficient in a two-dimensional (2D) adsorbate populating a square lattice of adsorption sites with strong adatom-adatom repulsive nearest-neighbor interactions. Results are valid below the critical temperature for coverages at which the adsorbate is structurally ordered. Interactions between nonactivated particles as well as those between the activated one and its nonactivated neighbors are accounted for. The starting point is Markovian master equations for the kinetics of microscopic states of the system, controlled by jumps of adatoms between adsorption sites. The diffusion coefficient is extracted in the long wavelength and the thermodynamic limits from the diffusive eigenvalue of a microscopic rate matrix associated with the equations. The eigenvalue is evaluated using an Anzatz for the left and the right eigenvectors of the matrix with the adsorbate ordering inscribed into their structure. The results are validated by Monte Carlo simulations of the diffusion process.

DOI: 10.1103/PhysRevB.72.235425 PACS number(s): 66.30.Pa, 02.50.Ga, 68.43.Jk, 66.10.Cb

I. INTRODUCTION

The collective or chemical diffusion coefficient for an adsorbate on a single-crystal surface depends on the adsorbate density (coverage) due to lateral interactions between diffusing particles.[1,2] Collective diffusion is a complicated many-body problem encountering many mathematical difficulties which, with a few exceptions, is usually studied using a variety of Monte Carlo simulation methods. Early efforts were summarized in a classical review by Gomer[1] and, more recently, by Danani *et al.*[3] and Ala-Nissila *et al.*[4] Kreuzer's work[5–7] stands here a bit apart in this respect that, using a kinetic lattice gas model, it is mainly interested in the adsorption and desorption kinetics in the presence of surface diffusion. In this analytic approach the kinetics is described by a hierarchy of kinetic equations for many-site correlation functions with several truncation schemes being designed to close the hierarchy. This is only one example of surface diffusion being important for other surface processes. The effectiveness of the surface mobility in relation to that of adsorption, desorption, chemical reactions, etc., determines catalytic activity of the surface.[8,9] Surface diffusion is of interest in nanostructuring because cluster surface diffusion enabling them to form islands controls growth of nanostructures from beam deposited clusters.[10] The experimental progress in this field is reviewed in Refs. 11–13.

Usually, one distinguishes between two types of interparticle interactions:[2] the interaction between nonactivated particles (ground state interactions) affecting thermodynamic properties of the adsorbate, and the interaction of the activated particle with adjacent nonactivated ones which affect the kinetics of diffusion only. One of the consequences of the ground state interactions is a formation, below a critical temperature, of ordered phases in the adsorbate. Relevant to this work is the simplest case of nearest-neighbor repulsive interactions between particles adsorbed on a square lattice of adsorption sites. Here, the system exhibits a continuous phase transition from a disordered to a staggered checkerboard $c(2\times 2)$ structure [illustrated later in Eq. (6), see, e.g., Ref. 14 for an example of the relevant phase diagram]. The ground state interactions—along with the interactions in the activated state—affect also kinetics of diffusion directly. The distinct role which kinetics and thermodynamics play in diffusion is often emphasized by writing the collective diffusion coefficient as a product,[1,15]

$$D(\theta) = D_J(\theta)\left(\frac{\partial(\mu/k_BT)}{\partial \ln \theta}\right)_T, \tag{1}$$

of the jump rate diffusion coefficient $D_J(\theta)$, accounting for the effective jump kinetics in the interacting system, and a "thermodynamic factor" directly related to the equilibrium mean square particle number fluctuation.

Diffusion on a lattice has a theoretical advantage over diffusion in continuous systems in this respect that there exists a separation of time scales between the elementary transition processes (atomic jumps between lattice sites here) and the time lapse between successive transitions, the sequence of which leads to the observed diffusion phenomena: the individual transitions take generally much less time than it takes to wait for the next step. This allows one to treat one atomic jump at a time, considering them to be statistically independent invoking effectively the Markovian hypothesis that the present state of the system is fully determined by its state at one past time rather than by its entire past history. As a consequence the kinetics of the microscopic states of the system is described by a Markovian master equation which is the starting point in our considerations. In our work we do

not invoke the factorization embodied in Eq. (1) because, in principle, with appropriate atomic jump rates determined by instantaneous interactions of the hopping atom with its neighbors (determined by an independent theoretical modeling) such an approach should result in a coverage dependent diffusion coefficient which automatically accounts for both factors in Eq. (1): the equilibrium properties of the system (including possible structural order) and the coverage dependent effective jump kinetics. In contrast to our work, however, a separate treatment of kinetic and equilibrium properties, embodied in Eq. (1), is the starting point in a majority of theoretical approaches so far. Relevant in this context is the work by Chumak and Uebing[16] in which the coverage dependence of the collective diffusion coefficient in the $c(2\times2)$ structure is derived for coverages around $\theta=0.5$ in an approach based on the factorization in Eq. (1). We will provide in Sec. III C a detailed comparison of the results of our approach with those of Ref. 16.

Our goal is to apply an approximate analytic method allowing us to derive the coverage dependent diffusion coefficient in a two-dimensional lattice gas of atoms strongly repelling its neighbors adsorbed at nearest-neighbor sites. In the method, designed and applied recently to one-dimensional lattice gas,[17] we avoid factorizing *a priori* the diffusion coefficient into its kinetic and thermodynamic part and avoid also introducing the multisite correlation functions. Instead, we extract the diffusion coefficient directly from the Markovian kinetics of the microscopic states of the gas by evaluating the diffusive eigenvalue of the microscopic master equation rate matrix. The eigenvalue is evaluated after variational forms of diffusive eigenvectors of this matrix (the left and the right one) are postulated. Equilibrium correlations and the structural phase of the adsorbate at a given temperature and coverage are incorporated into the postulated form of the vectors. For the $c(2\times2)$ phase below the critical temperature an algebraic expression for the coverage dependent collective diffusion coefficient is derived for coverages both below and above $\theta=0.5$ (i.e., down to and up to but not at or across the phase transition line). A discontinuity of $D(\theta)$ at $\theta=0.5$ is predicted. The discontinuity is, in fact, spurious and due to a partial neglect of thermal density fluctuations at $\theta=0.5$ in the postulated form of the eigenvectors but the analytic results agree very well with the results of Monte Carlo simulations, which predict a sharp, almost discontinuous variation of $D(\theta)$ across $\theta=0.5$. Our results complement the results of Ref. 16 obtained using an entirely different approach.

The paper is organized as follows. The theoretical model and the solution method are described in Sec. II. Detailed application for the $c(2\times2)$ structure follows in Sec. III and the results, discussion, and comparison with the simulation results are given in Sec. IV. Section V is devoted to conclusions and final remarks. Some material, not essential to follow the main line of the paper, is relegated to two appendixes.

II. THEORY

A. The system

We consider a square lattice of $L\times L$ adsorption sites. The lattice constant is a and periodic boundary conditions with a periodicity La are implied. The gas consists of N adsorbed atoms which may hop between neighboring adsorption sites. For an isolated adsorbed atom the potential energy landscape has minima V_g at the adsorption sites. If the potential energy at bridge sites—halfway between the adsorption sites—is V_s, then the transition rate for an atomic hopping between the neighboring adsorption sites is $W=\nu_0\exp[-\beta(V_s-V_g)]$ to be referred to as an isolated atom hopping rate. It is the same for the hops in both directions between two such sites.

When N is of the same order as L^2 then the hopping rates are modified due to the interactions between the hopping atom and other adsorbed atoms in its neighborhood. In this work we assume that only atoms at sites nearest to the adsorption site from which the hopping occurs and nearest to the bridge site over which the atom jumps affect the hopping rate by modifying the potential energies V_g and V_s of the hopping atom at these positions by J and J' per present neighbor, respectively. J and J' contribute to the interaction of the hopping atom in its ground and activated state, respectively. The thermodynamic equilibrium properties are affected by J only but the kinetics, i.e., the hopping rates are modified by both types of interactions. The energy corrections are assumed to be additive, for example, the correction at the initial adsorption site is $2J$ if there are two occupied adsorption sites nearest to the site from which the jump occurs. The maximum energy correction is $3J$ and $4J'$ for the hopping atom in the ground and the activated state, respectively. In the simplest case of the hopping atom interacting with only one other adsorbed neighbor we have three possibilities,

$$W_1^0=\frac{W}{\gamma},\ \text{for}\quad \begin{matrix}\circ & \circ & \\ \bullet & \bullet & \rightarrow\ \circ\\ \circ & \circ & \end{matrix}, \tag{2a}$$

$$W_0^1=W\sigma,\ \text{for}\quad \begin{matrix}\circ & \circ & \bullet\\ \circ & \bullet & \rightarrow\ \circ\\ \circ & \circ & \end{matrix}, \tag{2b}$$

$$W_1^1=\frac{W\sigma}{\gamma},\ \text{for}\quad \begin{matrix}\circ & \bullet & \circ\\ \circ & \bullet & \rightarrow\ \circ\\ \circ & \circ & \end{matrix}, \tag{2c}$$

in which, respectively, only the energy at the initial adsorption site is modified by J [Eq. (2a)], only the energy at the bridge site is modified by J' [Eq. (2b)], and both energies are modified [Eq. (2c)]. The factors

$$\gamma=e^{-\beta J},\quad \sigma=e^{-\beta J'}, \tag{3}$$

account for the modifications of the rates due to the extra interaction energy at the adsorption and at the bridge site, respectively. Note that W_0^1 is the rate of the jump from the configuration shown in Eq. (2b) to the one shown in Eq. (2c) while the hopping in the reverse direction occurs at the rate W_1^1. The hopping in the direction opposite to that in Eq. (2a) occurs at the rate $W_0^0=W$. In general, the hopping rates in this interaction model can be written as

$$W_n^m = W\frac{\sigma^m}{\gamma^n}, \quad m=0,\ldots,4, \quad n=0,\ldots,3. \tag{4}$$

We further restrict our model by assuming strong repulsive interactions between neighboring adsorbed atoms, i.e., $J>0$ so at sufficiently low temperatures we have

$$\frac{W_0^0}{W_1^0} = \frac{W_0^1}{W_1^1} = \gamma \ll 1. \tag{5}$$

Consequently, in equilibrium, the number of pairs of atoms adsorbed at neighboring adsorption sites is minimized. At half coverage ($\theta=N/L^2=0.5$) the lattice gas is organized into a staggered "checkerboard" order in which the occupied and the empty sites form two interpenetrating sublattices,

$$\begin{array}{ccccccc} \circ & \bullet & \circ & \bullet & \circ & \bullet & \circ \\ \bullet & \circ & \bullet & \circ & \bullet & \circ & \bullet \\ \circ & \bullet & \circ & \bullet & \circ & \bullet & \circ \\ \bullet & \circ & \bullet & \circ & \bullet & \circ & \bullet \\ \circ & \bullet & \circ & \bullet & \circ & \bullet & \circ \\ \bullet & \circ & \bullet & \circ & \bullet & \circ & \bullet \\ \circ & \bullet & \circ & \bullet & \circ & \bullet & \circ \end{array} \tag{6}$$

each with a lattice constant $\sqrt{2}a$. We refer to these sublattices as the F (filled, •) and the E (empty, ◦) ones. Each of them consists of $L^2/2$ sites. The checkerboard configuration is stable because the ratio of a hopping rate of an atom away from its regular position to the rate of a return jump is $W_0^2/W_3^2=\gamma^3\ll 1$. The checkerboard configuration is the starting point for our considerations of the coverage dependence of diffusion in an adsorbate with the long range staggered order. The equilibrium properties are not affected by the activated atom interactions with its neighbors so, formally, there is no restriction on J' (i.e., σ) and this is assumed throughout our work. Physically, however, the most likely case is that of $\sigma<\gamma$ because it is expected that the repulsion is stronger at shorter distances.

B. The method

The hopping rates appear in the microscopic Markovian master equations[6,7,18] for the probability $P(\{c\},t)$ that a microstate $\{c\}$ of a lattice gas occurs at time t

$$\frac{d}{dt}P(\{c\},t) = \sum_{\{c'\}}[W(\{c\},\{c'\})P(\{c'\},t) - W(\{c'\},\{c\})P(\{c\},t)]. \tag{7}$$

Here $W(\{c\},\{c'\})$ denotes a transition probability per unit time that the microstate $\{c'\}$ changes into $\{c\}$ due to an atomic jump of an atom from an occupied site to an unoccupied neighboring site—a particular $W(\{c\},\{c'\})$ is equal to one of the hopping rates described above (or is equal to zero if $\{c\}$ and $\{c'\}$ cannot be connected to each other by a hopping of a single atom). Effectively, the sum over $\{c'\}$ runs over all such microstates from which the microstate $\{c\}$ can be reached [the first term on the right-hand side of Eq. (7)] or which can be reached from $\{c\}$ (the second term).

For a system of N atoms distributed among L^2 sites we identify a microstate $\{c\}$ as follows:[17]

$$\{c\} = [\mathbf{X};\mathbf{m}_1,\mathbf{m}_2,\ldots,\mathbf{m}_{N-1}] \equiv [\mathbf{X};\{\mathbf{m}\}] \tag{8}$$

where $\mathbf{X}$ is a position of one of the atoms, referred to as the reference atom, and $\mathbf{m}_i$ is a set of two integers which identify a position, in multiples of the two fundamental lattice translation vectors, of the ith atom with respect to the reference atom. The set $\{\mathbf{m}\}=[\mathbf{m}_1,\mathbf{m}_2,\ldots,\mathbf{m}_{N-1}]$ is referred to as a configuration—it accounts for the relative geometrical arrangement of atoms in a given microstate. The transition rate does not depend on the positions of the reference atom in both configurations but only on the local environment of the jumping atom so $W(\{c\},\{c'\})=W_{\{\mathbf{m}\},\{\mathbf{m}'\}}$. This allows one to take the lattice Fourier transform

$$f(\mathbf{k}) = \sum_X e^{i\mathbf{k}\cdot\mathbf{X}} f(\mathbf{X}) \tag{9}$$

of the rate equations. Arranging lattice Fourier transforms $P_{\{\mathbf{m}\}}(\mathbf{k},t)$ of the probabilities $P(\{c\},t)\equiv P_{\{\mathbf{m}\}}(\mathbf{X},t)$ into a one-column array $\mathbf{P}(k,t)$ we get the $\mathbf{k}$-space rate equations which can be collectively written in a matrix form:

$$\frac{d}{dt}\mathbf{P}(\mathbf{k},t) = \mathbb{M}(\mathbf{k})\cdot\mathbf{P}(\mathbf{k},t), \tag{10}$$

where $\mathbb{M}(\mathbf{k})$, referred to as a rate matrix, is non-Hermitian due to the fact that the hopping rate from $\{c\}$ to $\{c'\}$ is not necessarily equal to that in the opposite direction. Its matrix elements are

$$M_{\{\mathbf{m}\},\{\mathbf{m}'\}}(\mathbf{k}) = F_{\{\mathbf{m}\},\{\mathbf{m}'\}}(\mathbf{k})W_{\{\mathbf{m}\},\{\mathbf{m}'\}} - \delta_{\{\mathbf{m}\},\{\mathbf{m}'\}}\sum_{\{\mathbf{m}''\}} W_{\{\mathbf{m}''\},\{\mathbf{m}\}}. \tag{11}$$

The first term is nonzero only when the configuration $\{\mathbf{m}\}=\mathbf{m}_1,\mathbf{m}_2,\ldots,\mathbf{m}_{N-1}$ is obtained from $\{\mathbf{m}'\}=\mathbf{m}'_1,\mathbf{m}'_2,\ldots,\mathbf{m}'_{N-1}$ as a result of a jump of a single atom by $\mathbf{a}$. When the jumping atom is the reference atom, then all vectors in both sets differ by $\hat{\mathbf{a}}=\mathbf{a}/a$: $\{\mathbf{m}'\}\equiv\{\mathbf{m}+\hat{\mathbf{a}}\}=\mathbf{m}_1+\hat{\mathbf{a}},\ldots,\mathbf{m}_i+\hat{\mathbf{a}}+\cdots+\mathbf{m}_{N-1}+\hat{\mathbf{a}}$ and then

$$F_{\{\mathbf{m}\},\{\mathbf{m}'\}}(\mathbf{k}) = \exp(i\mathbf{k}\cdot\mathbf{a}). \tag{12a}$$

When, however, the jumping atom is not the reference atom but, say, the one with the label ℓ, then $\{\mathbf{m}'\}=\mathbf{m}_1,\ldots,\mathbf{m}_\ell+\hat{\mathbf{a}},\ldots,\mathbf{m}_{N-1}$ and

$$F_{\{\mathbf{m}\},\{\mathbf{m}'\}}(\mathbf{k}) = 1. \tag{12b}$$

The diffusion coefficient is evaluated as

$$D(\theta) = \lim_{k\to 0}\frac{\lambda(\mathbf{k})}{k^2}, \tag{13}$$

where $-\lambda(\mathbf{k})$ is the diffusive eigenvalue of the $\mathbf{k}$-space rate matrix $\mathbb{M}(\mathbf{k})$. The diffusive eigenvalue is, by definition, the eigenvalue that vanishes in the $k\to 0$ limit. Formally, it can be evaluated from[17]

$$-\lambda(\mathbf{k}) = \frac{\tilde{\mathbf{e}}(\mathbf{k}) \cdot \mathbb{M}(\mathbf{k}) \cdot \left[\mathbf{P}^{\mathrm{eq}} \tilde{\mathbf{e}}^{\dagger}(\mathbf{k})\right]}{\tilde{\mathbf{e}}(\mathbf{k}) \cdot \left[\mathbf{P}^{\mathrm{eq}} \tilde{\mathbf{e}}^{\dagger}(k)\right]} \equiv \frac{\mathfrak{M}(\mathbf{k})}{\mathfrak{N}(\mathbf{k})}, \qquad (14)$$

where $\tilde{\mathbf{e}}(\mathbf{k})$ is the left eigenvector of $\mathbb{M}(\mathbf{k})$ corresponding to the eigenvalue $\lambda(\mathbf{k})$. The right eigenvector is[17,19] $[\mathbf{P}^{\mathrm{eq}} \tilde{\mathbf{e}}^{\dagger}(k)]$ where $\mathbf{P}^{\mathrm{eq}}$ is the right eigenvector of $\mathbb{M}(0)$ corresponding to the eigenvalue $\lambda(0)=0$. $[\mathbf{P}^{\mathrm{eq}} \tilde{\mathbf{e}}^{\dagger}]$ denotes a one-column array with components being products of the corresponding components of $\mathbf{P}^{\mathrm{eq}}$ and $\tilde{\mathbf{e}}^{\dagger}$. Physically, the $\{\mathbf{m}\}$-th component of $\mathbf{P}^{\mathrm{eq}}$ is (up to a common to all multiplicative factors) equal to the probability with which the configuration $\{\mathbf{m}\}$ occurs in the lattice gas in equilibrium.

Equation (14) for the diffusive eigenvalue is exact and in our approach it is approximated[17] by doing "variational" substitutions

$$\mathbf{P}^{\mathrm{eq}} \to \mathbf{P}^{\mathrm{v}},$$

$$\tilde{\mathbf{e}}^{\dagger}(\mathbf{k}) \to \mathbf{\Phi}^{\mathrm{v}}(\mathbf{k}), \qquad (15)$$

in it. Before doing this, one can use Eq. (11) and the detailed balance condition

$$W_{\{\mathbf{m}\},\{\mathbf{m}'\}} P^{\mathrm{eq}}_{\{\mathbf{m}'\}} = W_{\{\mathbf{m}'\},\{\mathbf{m}\}} P^{\mathrm{eq}}_{\{\mathbf{m}\}} \qquad (16)$$

to transform the numerator in Eq. (14) to a more convenient form from which the variational substitutions yield

$$\mathfrak{M}(\mathbf{k}) = \sum_{\{m\},\{\mathbf{m}'\}}^{\text{no rep}} W_{\{\mathbf{m}\},\{\mathbf{m}'\}} P^{\mathrm{v}}_{\{\mathbf{m}'\}} \times |F_{\{\mathbf{m}\},\{\mathbf{m}'\}}(\mathbf{k}) \Phi^{\mathrm{v}}_{\{\mathbf{m}'\}}(\mathbf{k}) - \Phi^{\mathrm{v}}_{\{\mathbf{m}\}}(\mathbf{k})|^2. \qquad (17)$$

Here "no rep" above Σ means that each configuration pair $\{\mathbf{m}\},\{\mathbf{m}'\}$ for which $W_{\{\mathbf{m}\},\{\mathbf{m}'\}} \neq 0$ appears in the sum only once: Eq. (17) automatically accounts for atomic jumps both from $\{\mathbf{m}\}'$ to $\{\mathbf{m}\}$ and back. With the variational substitutions the denominator in Eq. (14) becomes

$$\mathfrak{N}(\mathbf{k}) = \sum_{\{m\}} P^{\mathrm{v}}_{\{\mathbf{m}\}} |\phi^{\mathrm{v}*}_{\{\mathbf{m}\}}(\mathbf{k})|^2. \qquad (18)$$

In principle, the dependence on coverage $\theta=N/L^2$ is obtained by evaluating $\lambda(\mathbf{k})$ for N atoms distributed among L^2 sites of the square lattice respecting restrictions imposed on $\mathbf{k}$ due to the periodic boundary conditions and taking the thermodynamic limit ($L\to\infty, N\to\infty, N/L^2=\theta=\text{const}$) only at the end.

1. Variational substitutions

The choice of $\mathbf{P}^{\mathrm{v}}$ and $\mathbf{\Phi}^{\mathrm{v}}(\mathbf{k})$, the variational candidates for $\mathbf{P}^{\mathrm{eq}}$ and $\tilde{\mathbf{e}}^{\dagger}(\mathbf{k})$ respectively, must be dictated by physical considerations and opens the possibility of accounting for diffusion in adsorbates with long range order. Considerations concerning the choice of $\mathbf{P}^{\mathrm{v}}$ are simpler because they are based on equilibrium properties (embodied in the detailed balance conditions) only. Consequently, components of $\mathbf{P}^{\mathrm{v}}$ may depend on J (i.e., γ) but not on J'. Low temperature structural ordering of the adsorbate should be incorporated into the structure of $\mathbf{P}^{\mathrm{v}}$'s.

Considerations leading to the choice of $\mathbf{\Phi}^{\mathrm{v}}(\mathbf{k})$ are less intuitive. In principle, both types of interactions, J and J', should appear in it. An important formal requirement[17] is that for $k\to 0$ the components of $\mathbf{\Phi}^{\mathrm{v}}(\mathbf{k})$ should differ from each other only by terms linear in k in order to assure that the evaluated approximate $-\lambda(\mathbf{k})$ vanishes like k^2 in this limit—the condition which the diffusive eigenvalue must satisfy. Considerations may start with the "noninteracting" lattice gas in which rates of all atomic jumps, except those disallowed by the site blocking, are the same. The rate matrix in such a case is Hermitian and its diffusive eigenvectors are known:[17] the left and the right eigenvectors are $\tilde{\mathbf{e}}(\mathbf{k}) = \mathbf{\Phi}^{\dagger}(\mathbf{k})$ and $\mathbf{\Phi}(\mathbf{k})$, respectively, with the latter being a one–column array with components

$$\Phi_{\mathbf{m}_1,\mathbf{m}_2,\ldots,\mathbf{m}_{N-1}}(\mathbf{k}) \equiv \Phi_{\{\mathbf{m}\}}(\mathbf{k}) = 1 + \sum_{i=1}^{N-1} e^{-ia\mathbf{k}\cdot\mathbf{m}_i}. \qquad (19)$$

Each component is a sum of phase terms due to all occupied sites (the first term corresponds to the site occupied by the reference atom). In fact, in all our applications[17,20] so far, in which the structural ordering of the adsorbate did not occur, either because the gases considered were one-dimensional or because the temperature was high, we have used $\mathbf{\Phi}(\mathbf{k})$ given in Eq. (19) as a variational candidate $\mathbf{\Phi}^{\mathrm{v}}(\mathbf{k})$ in Eqs. (17) and (18) together with components of $\mathbf{P}^{\mathrm{v}}$ suggested by the detailed balance conditions.

In the present case of a two-dimensional (2d) structurally ordered lattice gas at low temperature, Eq. (19) no longer provides an appropriate candidate for $\mathbf{\Phi}^{\mathrm{v}}(\mathbf{k})$. In short, for the ordered phase, different occupation patterns around the hopping atom lead to a hierarchy of configurations: from the "primary" ones having the largest equilibrium probability, through less probable "secondary" ones to the "marginal" ones with negligibly small equilibrium probabilities (details are provided in the following section). While the marginal configurations may be ignored and Eq. (19) is an adequate anzatz for the components of $\mathbf{\Phi}^{\mathrm{v}}(\mathbf{k})$ corresponding to the primary configurations, the components corresponding to the secondary configurations, which also need to be accounted for, must be chosen taking into account their transient character [cf. Eqs. (24) and (26)]. Effectively, $\mathbf{\Phi}^{\mathrm{v}}(\mathbf{k})$ used in this work for the low temperature structurally ordered 2D adsorbate is essentially different from that used in a nonordered case, it does depend on both J and J' and leads to a prediction of the behavior of $D(\theta)$ around $\theta=0.5$ which is confirmed by independent theoretical considerations. This would not be possible for an anzatz which does not distinguish between transient and quasistationary configurations.

III. APPLICATION

A. $\theta > 0.5$

In order to explain the procedure used to evaluate the numerator $\mathfrak{M}(\mathbf{k})$ and the denominator $\mathfrak{N}(\mathbf{k})$ in Eq. (14) we consider first the case of $\theta > 0.5$. The case of $\theta < 0.5$ is then treated in an analogous manner, as we shall argue later. The number of atoms is $N=L^2/2+\delta N$ and the extra δN atoms are

adsorbed at the sites of the E sublattice. Any configuration obtained in this way is referred to as a "primary configuration": in it, all $L^2/2$ sites of the F sublattice and δN sites of the E sublattice are filled. The only unoccupied sites are in the E sublattice. The equilibrium probabilities of the primary configurations are equal to each other because extra atoms in the E sublattice interact only with the nearest neighbors in the F sublattice but do not interact among themselves. Components of $\mathbf{P}^{\nu}$ corresponding to the primary configurations are set to be equal to 1. Another class of configurations, referred to as "secondary," consist of such configurations, which are obtained from the primary ones by moving one of the $L^2/2$ atoms from its regular position in the F sublattice to the neighboring empty site in the E sublattice. Here, $L^2/2-1$ (all but one) sites of the F sublattice and $\delta N+1$ sites of the E sublattice are filled. The equilibrium probabilities of the secondary configurations are determined using the detailed balance condition: the secondary configuration components of $\mathbf{P}^{\nu}$ are equal to the ratio of the primary-to-secondary configuration jump rate to the jump rate in the opposite direction. Further jumps may result either in a configuration of a primary type or a configuration in which all but two (or more) sites in the F sublattice and $\delta N+2$ (or more) sites in the E sublattice are filled. Such configurations are referred to as "marginal."

To be specific we list now all possible types of atomic jumps between the primary and the secondary configurations. For each of them we show in the diagrams to follow both configurations, a primary and a secondary one, involved. We show only a fragment of the lattice around the atom, which hops between two sites in a central row. An occupation state of the remainder of the lattice is the same for both members of each pair and has all sites of the F sublattice and up to δN sites of the E sublattice filled with the remaining sites of the E sublattice unoccupied. The lattice sites (in either sublattice) which are filled by atoms are represented by •'s. We label the primary (at the left-hand side) and the secondary (at the right-hand side) configurations by A_n and A_n^*, respectively, where n is the number of extra atoms, represented also by •'s, occupying these sites of the E sublattice that are close enough to the hopping atom (easy to identify by comparing A_n with A_n^*) to influence its jump rates. We use a prime ($'$) to distinguish between geometrically inequivalent configurations corresponding to the same n. The sites of the E sublattice, which must remain unoccupied in the configurations shown are represented by ∘'s while ⊗'s represent more distant sites of the E sublattice whose occupation state does not affect the jump rate of the hopping atom: they are either empty or filled by some of the extra atoms. The jump rates are fully determined by the occupation state of the sites which in A_0 in Eq. (20a) are represented by ∘'s. These four sites form the "active cell," which will be used later on. n of these four sites are filled in the primary configurations A_n. The ⊗ sites can be filled by some of the remaining $\delta N-n$ extra atoms or be empty. The jump rates in each direction are listed between the configurations shown. They satisfy the detailed balance conditions involving components of $\mathbf{P}^{\nu}$ which are given below the configurations (they are equal to 1 for all primary configurations). The jump of the hopping atom, which transforms the primary configuration A_n into the secondary one, A_n^*, will be referred to as the "primary jump."

Thus when all the δN extra atoms are far enough from the hopping atom then we have $n=0$ and the transition rates are determined only by the nearest atoms residing in the F sublattice. We have

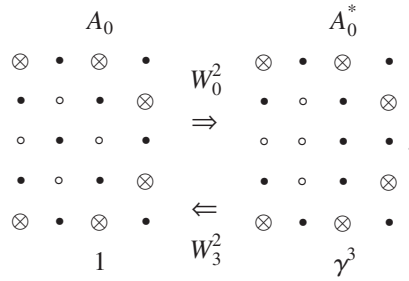

(20a)

For $n=1$ we have two generic cases:

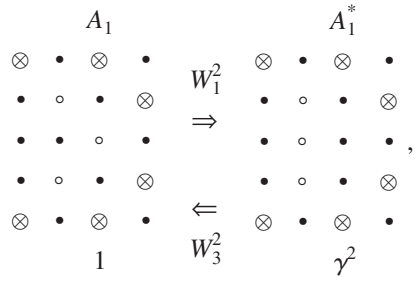

(20b)

and

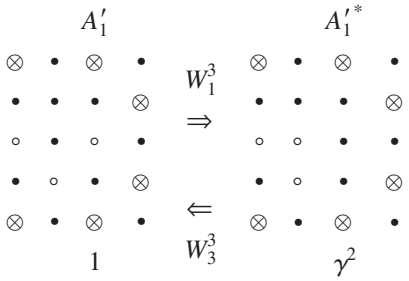

(20c)

with the nearest extra atom in the E sublattice situated, respectively, on or off the line along which the atomic jump occurs. In the configurations A_1 and $A_1'^*$ the extra atom is placed above the line along which the atomic jump occurs and one has to consider also configurations with the atom placed below this line. Similarly, the generic cases for $n=2$ are

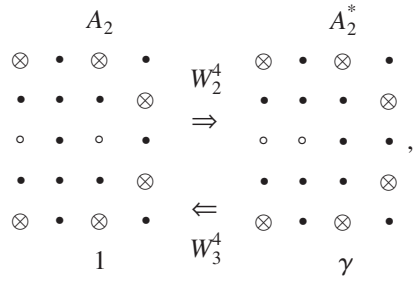

(20d)

and

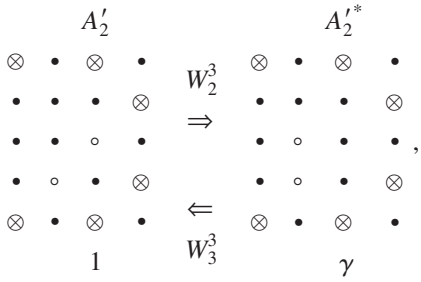

(20e)

plus configurations in which one of the extra atoms is below the jump line. For $n=3$ the primary and the secondary configurations are equally probable:

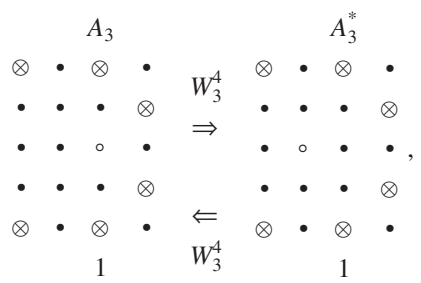

(20f)

Note that the configurations A_3 and A_3^* occur with the same probability because the jump rates in both directions are the same. In fact, the configuration A_3^* is as primary as A_3 and this is an important point which will be ignored here. We will return to this in Sec. IV where the results of our approach are confronted with the results of computer simulations. Returning to Eq. (20) we note that only diagrams for the primary jumps in the horizontal direction from left to right are shown. Similar diagrams have to be considered for the leftward, upward, and downward primary jumps. There are 32 cases in total. In what follows we will introduce a label α having 32 values: A_0, A_1, A_1', etc. to refer to all types of pairs of the primary and secondary configurations. Then, W_α denotes the corresponding transition rate for the primary jump [there are only six different W_α's, as listed in Eqs. (20)].

Note that the diagrams in Eq. (20) list all possible atomic jumps between primary and secondary configurations. One might argue that, for example, a jump of the third atom in the second row (counting from the top or bottom) in the configuration A_3 to the right and back is another possible transition between a primary and a secondary configuration, not considered in Eq. (20). This is not the case: it belongs to the $A_1 \Leftrightarrow A_1^*$ class listed in Eq. (20b). The two extra atoms present in the A_3 diagram do not affect the rate of this jump in either direction and their presence is accounted for in the environmental factor (to be defined shortly) associated with the A_1 configuration.

Summations in $\mathfrak{M}(\mathbf{k})$ and $\mathfrak{N}(\mathbf{k})$, Eqs. (17) and (18), respectively, are weighted by their probabilities specified in $\mathbf{P}^{\mathrm{v}}$. For $\gamma \ll 1$ the contributions due to the secondary and the marginal configurations can be ignored in $\mathfrak{N}(\mathbf{k})$, effectively reducing it to the expression analogous to that considered in Ref. 17—we will return to it later.

The summation in $\mathfrak{M}(\mathbf{k})$ in Eq. (17) runs over pairs of configurations connected by a jump of one atom in either direction. Therefore we have contributions due to the primary-secondary configurations (i.e., the primary jumps and back), the contributions due to transitions in either direction between the secondary and the marginal configurations with $\delta N+2$ sites in the E sublattice filled, the contributions due to transitions between these marginal configurations and the marginal configurations with $\delta N+3$ in the E sublattice filled, and so on. For $\gamma \ll 1$ the contributions due to the primary-secondary configuration pairs dominate over contributions due to configuration pairs involving one or two marginal configurations. For example, one can easily check that contributions due to the transitions between any A_0^* configuration and all possible marginal configurations reached from them are γ^{-2} or even γ^{-3} times smaller than contributions due to the $A_0 \Leftrightarrow A_0^*$ transitions. For $A_1'^*, A_2^*, A_2'^*$, and A_3^* the contributions due to the transitions to marginal configurations are from γ^{-1} to γ^{-3} times smaller than those involving transitions to and from the primary configurations. Consequently, only contributions due to pairs of configurations listed in Eq. (20) are kept in $\mathfrak{M}(\mathbf{k})$ from now on.

To avoid double counting of the pairs involved in the summation we associate $\{\mathbf{m}'\}$ and $\{\mathbf{m}\}$ in Eq. (17) with the primary and the secondary configurations, respectively, so $P^{\mathrm{v}}_{\{\mathbf{m}\}'}=1$. Note that the set $\{\mathbf{m}\}$, specifying a particular configuration, is a set of vectors $\mathbf{m}_i$ identifying positions of all $N-1$ atoms with respect to the reference atom. Considerations similar to those presented in Ref. 17—in which an important role is played by the fact that $|F_{\{\mathbf{m}\},\{\mathbf{m}'\}}\Phi^{\mathrm{v}}_{\{\mathbf{m}'\}} - \Phi^{\mathrm{v}}_{\{\mathbf{m}\}}|$ is the same function of $\mathbf{k}$ for all pairs of configurations with identical local environments of the hopping atom no matter whether this atom is the reference atom [in which case F is given in Eq. (12a)] or any other atom (in which case $F=1$)—allow one to cast $\mathfrak{M}(\mathbf{k})$ into the following form:

$$\mathfrak{M}(\mathbf{k}) = -\sum_{\alpha} W_\alpha \mathfrak{D}_\alpha \mathcal{C}_\alpha(\mathbf{k}). \tag{21}$$

Here the summation is over all primary-secondary configuration pair types (32 in this case)—the original summation in Eq. (17) containing a macroscopic number of terms is reduced to a summation containing relatively few terms because, as explained in what follows, a macroscopic number of terms in the original summation contribute equally to it. W_α is the corresponding transition rate from the primary to the secondary configuration, and

$$\mathcal{C}_\alpha(\mathbf{k}) = \left|\Phi^{\mathrm{v}}_{\{\mathbf{m}'\}}(\mathbf{k}) - \Phi^{\mathrm{v}}_{\{\mathbf{m}\}}(\mathbf{k})\right|^2 = \left|\Phi^{\mathrm{v}}_{\alpha,\mathrm{prm}}(\mathbf{k}) - \Phi^{\mathrm{v}}_{\alpha,\mathrm{sec}}(\mathbf{k})\right|^2. \tag{22}$$

A use in the second line of Eq. (22) is made of the fact that $\mathcal{C}_\alpha(\mathbf{k})$ can be evaluated using a typical primary-secondary configuration pair $[\{\mathbf{m}'\},\{\mathbf{m}\}]$ corresponding to the transition rate W_α. Which particular pair is used to evaluate $\mathcal{C}_\alpha(\mathbf{k})$ is not relevant as long as the reference atom is not selected as the hopping atom in such a pair. Otherwise, $F_{\{\mathbf{m}\},\{\mathbf{m}\}'}$ would not be equal to 1 and would have to appear in Eq. (22) explicitly [cf. Eq. (12)].[21]

In fact, arriving at Eq. (21) another property of $\Phi^{\nu}_{\{\mathbf{m}\}}$'s is used from which it follows that only the truly local environment of the hopping atom, i.e., the geometrical arrangement of the n extra atoms occupying the sites of the E sublattice nearest to it, determines $\mathcal{C}_{\alpha}(\mathbf{k})$: it is identical for any two configuration pairs $[\{\mathbf{m}\},\{\mathbf{m}'\}]$ sharing the same local environment of the hopping atom even if they differ in the way in which the remaining $\delta N-n$ distant atoms added to the system are arranged. This is why the summation in Eq. (21) has only a few terms (32 in our case) in contrast to the original summation in Eq. (17) where the number of terms is macroscopically large. Instead, $\mathfrak{D}_{\alpha}$ is a macroscopically large number. This reduction in the number of summation terms is possible because the contributions due to the $\delta N-n$ distant extra atoms cancel out in the difference of Φ's in Eq. (22). Consequently, $\mathfrak{D}_{\alpha}$'s corresponding to a given rate W_{α} in Eq. (17) are identical. The cancellation is a quite obvious property of $\mathbf{\Phi}^{\nu}(\mathbf{k})=\mathbf{\Phi}(\mathbf{k})$ [cf. Eq. (19)] but it is one of the properties that any candidate for $\mathbf{\Phi}^{\nu}(\mathbf{k})$ should have.

The factor $\mathfrak{D}_{\alpha}$, referred to as the environmental factor, is equal to the total number of the configuration pairs of type α in the gas. To evaluate it we divide the entire lattice into two sublattices: the active cell and the environment. The active cell contains the site within the F sublattice filled by the hopping atom and $l=4$ adjacent sites of the E sublattice around it [shown as $\circ$ in the configuration A_0 in Eq. (20a)]. The hopping atom is referred to as a "participant." One of the E sites within the cell must be empty (in the primary configuration) to allow for the jump of the participant atom. The remaining three E sites are filled by $n=0$, 1, 2, or 3 atoms from the pool of the δN extra ones. The jump rates of the participant in either direction are affected only by the occupation state of these three sites within the cell, and they do not depend on the occupation state of the E sites within the environment (the ones shown as $\otimes$). The environmental factor is then equal to

$$\mathfrak{D}_{\alpha} \equiv \mathfrak{D}(l,n;L^2/2,\delta N) = \delta N\,! \begin{pmatrix} \frac{L^2}{2}-l \\ \delta N-n \end{pmatrix}, \tag{23}$$

with $n=0$, 1, 2, 3, and $l=4$ in our case. Here, the factor $\delta N!$ is due to the fact that all configurations differing only by a permutation of the extra atoms among the sites which they occupy are legitimate while the remaining factor counts all distinct configurations of the environment in which $\delta N-n$ atoms fill $L^2/2-l$ available sites of the E sublattice.

Further progress requires specification of the variational candidates for the components of $\mathbf{\Phi}^{\nu}(\mathbf{k})$ corresponding to the primary and the secondary configurations, to be used in Eq. (22). As already discussed in Sec. II B 1, the choice is dictated by intuition rather than hard rules and for the primary quasistationary configurations we choose

$$\Phi^{\nu}_{\{\mathbf{m}'\},\mathrm{prm}}(\mathbf{k}) = \Phi_{\{\mathbf{m}'\}}(\mathbf{k}), \tag{24}$$

with $\Phi_{\{\mathbf{m}'\}}(\mathbf{k})$ given in Eq. (19). Such an anzatz should be adequate for components corresponding to the most probable, quasistationary configurations. Each such component is a sum of phase terms $\exp(-ia\mathbf{k}\cdot\mathbf{m}'_j)$ due to all sites j occupied in the configuration $\{\mathbf{m}'\}$, exactly as in the case of a lattice gas without interactions. With Eq. (24) we can evaluate $\mathfrak{N}(\mathbf{k})$ defined in Eq. (18) because, as argued in the third paragraph following Eq. (20f), only the primary configurations contribute significantly to it. The resulting expression for $\mathfrak{N}(\mathbf{k})$ is very similar to the one dealt with in Appendix C of Ref. 17. The result is

$$\mathfrak{N}(\mathbf{k}) = \mathfrak{D}(2,1;L^2/2,\delta N) = \delta N\,! \begin{pmatrix} \frac{L^2}{2}-2 \\ \delta N-1 \end{pmatrix}. \tag{25}$$

It does not depend on $\mathbf{k}$ due to the periodic boundary conditions. Note that the factors $\delta N!$ in Eqs. (23) and (25) cancel out in the ratio $\mathfrak{M}/\mathfrak{N}$. We note here that the result in Eq. (25) does not account for a contribution $\mathfrak{N}(\mathbf{k})$ due to configurations A_3^*, which in this work are treated as if they were secondary ones while, in fact, their equilibrium probability is the same as that of the primary ones. Such omission in $\mathfrak{N}(\mathbf{k})$ is necessary for consistency because also in the numerator $\mathfrak{M}(\mathbf{k})$ the same assumption is used: atomic jumps initiated from A_3^* are ignored in Eq. (21) (cf. Sec. IV for further discussion).

For the components of $\mathbf{\Phi}^{\nu}(\mathbf{k})$ corresponding to the secondary configurations $\{\mathbf{m}\}$ in Eq. (22) we use an anzatz reflecting the transient character of these configurations. We propose

$$\Phi^{\nu}_{\{\mathbf{m}\},\mathrm{sec}}(\mathbf{k}) = \sum_{\{\mathbf{m}''\}}^{\mathrm{prm}} C_{\{\mathbf{m}\},\{\mathbf{m}''\}}\Phi_{\{\mathbf{m}''\}}, \tag{26}$$

where the sum is over all primary configurations $\{\mathbf{m}''\}$ (including the original $\{\mathbf{m}'\}$) from which the secondary configuration $\{\mathbf{m}\}$ can be reached as a result of a jump of a single atom. The coefficients $C_{\{\mathbf{m}\},\{\mathbf{m}''\}}$ add up to 1 and are proportional to the rates of transitions $W_{\{\mathbf{m}\},\{\mathbf{m}''\}}$ from the configuration $\{\mathbf{m}''\}$ to the configuration $\{\mathbf{m}\}$. Consequently, the phase terms $\exp(-ia\mathbf{k}\cdot\mathbf{m}_j)$ are not contributed in Eq. (26) by the sites which are occupied in the secondary (transient) configuration $\{\mathbf{m}\}$ itself but by the sites which are occupied in all primary quasistationary configurations which can be converted into the configuration $\{\mathbf{m}\}$ by a jump of one atom. These contributions are weighted by the appropriate jump rates. Note that the "variational" choice made in Eq. (26) can only be justified using plausibility arguments. It is argued in Appendix A, using an example of a random walk of a particle along the 1D chain of sites with alternating potential well depths, that any secondary configuration (corresponding to a particle trapped in the shallow well) component of the left eigenvector $\tilde{\mathbf{e}}$ of $\mathbb{M}(\mathbf{k})$ corresponding to the diffusive eigenvalue is expected to be an average of the phase terms associated with both primary configurations (a particle trapped in a deep well) from which the particular secondary configuration (shallow well) can be reached. Physically, the secondary configuration components of the density fluctuation, not necessarily present at $t=0$, are populated from the primary ones by fast transients long before diffusion sets in and restores the overall equilibrium. See the end of Appendix A for further clarifications of this point. Note that in contrast

to $\Phi^{\mathrm{v}}_{\{\mathbf{m}\},\mathrm{prm}}(\mathbf{k})$'s given in Eq. (24) the components $\Phi^{\mathrm{v}}_{\{\mathbf{m}\},\mathrm{sec}}(\mathbf{k})$ do depend on interactions J and J' between adatoms.

Before continuing with a detailed evaluation of all contributions to $\mathfrak{M}(\mathbf{k})$ we note that both $\Phi^{\mathrm{v}}_{\{\mathbf{m}\}}(\mathbf{k})$ and $\Phi^{\mathrm{v}}_{\{\mathbf{m}'\}}(\mathbf{k})$ in Eq. (22) can be multiplied by the same phase factor $\exp(i\mathbf{X}\cdot\mathbf{k})$ without affecting the result for $\mathcal{C}(\mathbf{k})$. Effectively, this multiplies $\Phi_{\{\mathbf{m}'\}}(\mathbf{k})$ and all $\Phi_{\{\mathbf{m}''\}}(\mathbf{k})$'s in Eqs. (24) and (26), respectively, by the same factor having, as seen from Eq. (19), an effect of merely shifting position of the reference atom by $\mathbf{X}$. Consequently, using $\Phi_{\{\mathbf{m}\}}(\mathbf{k})$'s in Eqs. (24) and (26) we can treat $\mathbf{m}_i$'s in $\{\mathbf{m}\}$ as absolute atomic positions of occupied sites with respect to a conveniently chosen fixed origin. To simplify the notation we introduce

$$f_{n,m} = e^{ia(k_y n + k_x m)}, \tag{27}$$

where (n,m) labels lattice positions within the active cell as follows:

$$\begin{array}{ccc} \bullet & (1,0) & \bullet \\ (0,\bar{1}) & (0,0) & (0,1) \\ \bullet & (\bar{1},0) & \bullet \end{array}. \tag{28}$$

Here, $\bar{1}$ means -1. The hopping atom resides at (0, 0) in the primary configurations. The remaining four labeled sites may be filled with up to three extra atoms or remain unoccupied: compare the diagram in Eq. (28) with the left-hand side diagrams in Eq. (20).

First of all, $\mathcal{C}_\alpha(\mathbf{k})=0$ for configurations $\alpha=A_0$ because the secondary configuration A_0^* in Eq. (20a) can only be obtained from one only primary configuration, A_0. Consequently, according to Eqs. (24) and (26), $\Phi^{\mathrm{v}}_{A_0,\mathrm{prm}}=\Phi^{\mathrm{v}}_{A_0,\mathrm{sec}}$. This takes care of the first four (due to four possible jump directions) out of the total of 32 terms in the sum in Eq. (21).

For $\alpha=A_1$, the secondary configuration A_1^* in Eq. (20b) can be obtained either from the primary configuration A_1 shown there or from another primary configuration, denoted $\hat{A}_1$, which differs from A_1 by having the extra atom at the position (0, 1) rather than at $(0,\bar{1})$. The rates from both primary configurations to the secondary A_1^* are the same (W_1^2) so, according to Eqs. (22) and (26) we get

$$\Phi_{A_1,\mathrm{sec}} = \frac{1}{2}(\Phi_{A_1} + \Phi_{\hat{A}_1}),$$

$$\mathcal{C}_{A_1}(\mathbf{k}) = \frac{1}{4}|\Phi_{A_1}(\mathbf{k}) - \Phi_{\hat{A}_1}(\mathbf{k})|^2 = \frac{1}{4}|f_{0,\bar{1}} - f_{0,1}|^2. \tag{29}$$

Equation (29) accounts for the situations in which the hopping atom jumps away from the extra atom in the direction to the right [as shown in Eq. (20b)]. The jumps to the left are accounted for by adding a term with the roles of the configurations A_1 with $\hat{A}_1$ interchanged (effectively multiplying $\mathcal{C}_{A_1}$ by 2). The jumps in the vertical direction are accounted for by then adding a term with the order of subscripts of f's reversed. In this way we get $\mathcal{C}_1(\mathbf{k})$—the sum of all four $\mathcal{C}_\alpha$'s corresponding to $n=1$ which in Eq. (21) will eventually be multiplied by W_1^2 and by $\mathfrak{D}(4,1;L^2/2,\delta N)$:

$$\mathcal{C}_1(\mathbf{k}) = \frac{1}{2}\left(|f_{0,\bar{1}} - f_{0,1}|^2 + |f_{\bar{1},0} - f_{1,0}|^2\right)$$
$$= 2(\sin^2(k_x a) + \sin^2(k_y a)) \to 2(ka)^2. \tag{30}$$

The limit is obtained for $ka \ll 1$ with $k^2 = k_x^2 + k_y^2$.

All the remaining cases are treated similarly and this is done in detail in Appendix B. Each of the diagrams in Eq. (20) allows one to evaluate several contributions to Eq. (21) for which the rate of the primary jump is the same. We have seen that four contributions corresponding to $n=0$ are strictly zero and that $\mathcal{C}_1$ in Eq. (30) evaluated from the diagram in Eq. (20b) accounts for four $n=1$ cases. The remaining eight $n=1$ cases are incorporated in $\mathcal{C}_1'$ evaluated in Eq. (B2) using the diagram in Eq. (20c). The $n=2$ diagrams in Eqs. (20d) and (20e) result in $\mathcal{C}_2$ [Eq. (B4)] and $\mathcal{C}_2'$ [Eq. (B6)], respectively, which account for four cases with the primary jump rate W_2^4 and for eight cases with the rate W_2^3, respectively. In both cases the same secondary configuration can be obtained from different primary ones through transitions with different jump rates. This makes $\Phi_{A_2,\mathrm{sec}}$ and $\Phi_{A_2',\mathrm{sec}}$ [Eqs. (B3) and (B5), respectively] somewhat more complicated than $\Phi_{A_1,\mathrm{sec}}$ or $\Phi_{A_1',\mathrm{sec}}$. This is the reason why $\mathcal{C}_2$ and $\mathcal{C}_2'$ contain σ accounting for the bridge site interactions. Finally, the $n=3$ diagram in Eq. (20f) allows one to evaluate $\mathcal{C}_3$ [Eq. (B8)], which accounts for four cases in which the primary jump rate is W_3^4. Here, the secondary configuration A_3^* is as probable as A_3 so Eq. (24) rather than Eq. (26) is used to evaluate $\Phi_{A_3,\mathrm{sec}}$.

We can now get $\mathfrak{M}(\mathbf{k})$ immediately from Eq. (21). To get $\lambda(\mathbf{k})$ and the collective diffusion coefficient it is necessary to divide by $\mathfrak{N}(\mathbf{k})$, take the thermodynamic limit $\delta N \gg 1, L^2 \gg 1$, and divide by k^2 [cf. Eq. (13)]. With Eqs. (23) and (25) and the definition

$$p \equiv 2\theta - 1 = \frac{\delta N}{L^2/2}, \tag{31}$$

we get the thermodynamic limit of the ratios

$$\frac{\mathfrak{D}(4,n;L^2/2,\delta N)}{\mathfrak{D}(2,1;L^2/2,\delta N)} \to p^{n-1}(1-p)^{3-n}, \tag{32}$$

for $n=1$, 2, 3. For $0.5 \leqslant \theta \leqslant 1$ we have $0 \leqslant p \leqslant 1$ but our approach breaks down considerably below $\theta=1$ at a coverage where the system loses its staggered order. The result for the diffusion coefficient is

$$D(\theta) = k^{-2}\{[\mathcal{C}_1(\mathbf{k})W_1^2 + \mathcal{C}_1'(\mathbf{k})W_1^3](1-p)^2 + [\mathcal{C}_2(\mathbf{k})W_2^4 + \mathcal{C}_2'(\mathbf{k})W_2^3]p(1-p) + \mathcal{C}_3(\mathbf{k})W_3^4 p^2\}. \tag{33}$$

With Eqs. (30), (31), (B2), (B4), (B6), and (B8), and the rates taken from Eq. (4) it becomes

$$D(\theta) = 2Wa^2\frac{\sigma^2}{\gamma}\left[4(1+\sigma)(1-\theta)^2 + 8\frac{1+\sigma}{2+\sigma} \times \frac{\sigma}{\gamma}(1-\theta)(2\theta-1) + \left(\frac{\sigma}{\gamma}\right)^2(2\theta-1)^2\right]. \tag{34}$$

The contribution proportional to $(1-\theta)^2$ is due to the $\alpha=A_1$ and $\alpha=A_1'$ [cf. Eqs. (30) and (B2), respectively] contributions

Eq. (21), both corresponding to $n=+1$. It dominates for coverages close to $\theta=0.5$ for which the microstates with extra atoms being well apart are most common. As the coverage increases, the microstates with extra atoms being so close to each other that two or even three of them affect the jump rates simultaneously become relatively more common. They are responsible for contributions proportional to $(1-\theta)(2\theta-1)$ (i.e., $n=+2$) and to $(2\theta-1)^2$ (i.e., $n=+3$), respectively. For $\sigma>\gamma$ the relative importance of these two contributions is increased by the extra factors σ/γ and $(\sigma/\gamma)^2$.

B. $\theta<0.5$

The procedure used in Sec. III A can be adopted for $\theta<0.5$ with minimal modifications. Now, the number of atoms in the system is $N=L^2/2-\delta N$, i.e., δN atoms are removed from the F sublattice. Treating the vacant sites as sites filled with holes we have δN sites of the F sublattice and all $L^2/2$ sites of the E sublattice filled with holes while the $L^2/2-\delta N$ sites of the F sublattice, occupied by atoms, are considered empty—they are not filled with holes. From now on all considerations made in the previous section apply—the role of atoms is played now by holes.

The environmental factors are still given in Eq. (23). This is obvious from their interpretation: they count the number of configurations of the environment containing $\delta N-n$ extra holes (in the F sublattice) while the active cell has n of them at fixed positions (times δN!). The denominator is also the same as for $\theta>0.5$, i.e., it is given in Eq. (25). It should not be surprising because, after all, the denominator is determined by geometry only. Detailed evaluation[17] shows that the exponentials $\exp(-i\mathbf{k}\cdot\mathbf{m}_i)$ in Eq. (19) can be tied with atoms at positions $\mathbf{m}_i$ with respect to the reference atom (as done in this paper) or, as well, can be tied to the positions of holes with respect to the reference hole. The result for the denominator $\mathfrak{N}$ is the same in both calculations provided the restrictions on $\mathbf{k}$'s due to the periodic boundary conditions are accounted for. In effect the result in Eq. (33) can be easily adapted when two modifications are made in it.

The first modification is easy. The net coverage is now $\theta=(L^2/2-\delta N)/L^2$ so p, defined by the first equality in Eq. (31), is now equal to $p=-\delta N/(L^2/2)$. Consequently, one has to change p to $-p$ on the right-hand side of Eq. (32) and in Eq. (33).

The other modifications necessary in Eq. (33) are due to the fact that the jump rates of "holes" are different than the jump rates of atoms—with some atoms removed, the jumping atoms have less chance to interact with their neighbors. With a proper redefinition of the symbols we can still use our diagrams in Eq. (20) to identify the jump rates. The holes are represented by •'s. The active cell is still formed by the sites represented by ◦'s in A_0 in Eq. (20a) but these sites have no holes now, i.e., they are occupied by atoms. Some of them contain holes in other configurations and are then shown as •. The sites represented by ⊗ also do not have holes at $\theta=0.5$ but in the system where n extra holes are created some of these sites are filled by $\delta N-n$ holes. As before, the occupation state of these sites is irrelevant for the jump rate. Identifying these rates, which replace the ones listed in Eq. (20), we must be aware that the interacting objects are the atoms, not holes. Consequently, the jump rates present in Eq. (33) must be changed as follows:

$$W_2^4, W_3^4 \to W_0^0 = W,$$

$$W_1^3, W_2^3 \to W_0^1 = W\sigma,$$

$$W_1^2 \to W_0^2 = W\sigma^2. \tag{35}$$

Note that none of the rates contain γ because the interactions do not modify the energy of the hopping atom in its initial site in primary configurations. It is convenient to *label* configurations with $n=1, 2, 3$ holes in the active cell using *negative* integers, i.e., the corresponding *labels* are $n=-1,-2,-3$ [these are labels only, so positive integer n should still be used in the modified Eq. (32)].

The modification of the jump rates also affect expressions for $\mathcal{C}_2(\mathbf{k})$ and $\mathcal{C}_2'(\mathbf{k})$. Namely, before using them in Eq. (33) one must replace σ with $1/\sigma$ in Eqs. (B4) and (B6). With all these changes we obtain

$$D(\theta) = 2Wa^2\left[4\sigma(1+\sigma)\theta^2 + 8\sigma\frac{1+\sigma}{2\sigma+1}\theta(1-2\theta) + (1-2\theta)^2\right], \tag{36}$$

applicable for $0\leqslant\theta\leqslant0.5$. This time, however, our approach breaks down for coverages below that at which the system loses its staggered order. The contribution proportional to θ^2 is due to microstates in which positions of missing atoms (from the configuration at $\theta=0.5$) are well apart so configurations corresponding to active cells with one missing atom (i.e., one hole) ($n=-1$) dominate the process. The other two terms, proportional to $(1-\theta)(2\theta-1)$ and to $(2\theta-1)^2$, gain importance as the coverage goes down and atomic jumps occurring in the neighborhood of, respectively, two or three atoms missing from the F sublattice become more common. In such a case the active cells corresponding to $n=-2$ and $n=-3$ cannot be ignored. In contrast to the case of $\theta>0.5$ the diffusion coefficient does not explicitly depend on γ, as already noted below Eq. (35). The implicit dependence is here, of course, because Eq. (36) is valid only when $\gamma\ll1$.

C. $\theta=0.5$ discontinuity

Before confronting theoretical predictions with the numerical simulation data we note that, except for $\sigma=\gamma$, the diffusion coefficient predicted by Eqs. (34) and (36) is a discontinuous function of θ at $\theta=0.5$. Such discontinuity was already noticed by Chumak and Uebing.[16] A persistent presence of such discontinuities in unpublished numerical simulations by one of the authors (M.Z.K.) was, in fact, one of primary motivations for developing the present analytic approach to diffusion. The discontinuity can be easily understood: when an atom is added to a perfect checkerboard structure (an extra atom in the E sublattice) at $\theta=0.5$, the jump rates controlling the atomic migration are W_1^2 and W_1^3, as listed in, respectively, Eqs. (20b) and (20c) (the return

rates in these equations are automatically obtained using the detailed balance condition incorporated in the appropriate components of $\mathbf{P}^{\mathrm{v}}$), while for an atom removed from this configuration the appropriate rates (corresponding to the migration of a hole in the F sublattice) are W_0^2 and W_0^1. In fact, the diffusion coefficient on both sides of $\theta=0.5$ can be evaluated exactly using the procedure applied by the authors to investigate oxygen migration on the Ru(001) surface.[22] This method, requiring considering seven different geometrical configurations of the extra atom/hole in the checkerboard structure, leads to a set of seven master equations from which the following expression for the diffusion coefficient is obtained:

$$D = 2Wa^2\frac{(1+\sigma)\sigma}{1+6\gamma^2}\begin{cases}1, & \text{for } \theta = 0.5^-\\ \dfrac{\sigma}{\gamma}, & \text{for } \theta = 0.5^+.\end{cases} \tag{37}$$

It agrees, for $\gamma \ll 1$, with the results in Eqs. (34) and (36) for $\theta=0.5$. We stress here that the result in Eq. (37) is an independent one, obtained using an approach unrelated to the variational method being the subject of this work. This approach, developed in Ref. 22, allows one to investigate low temperature collective diffusion at a particular coverage at which the system is perfectly ordered. The ability of reproducing this result by our variational approach is an independent consistency check confirming correctness of our variational choice, Eqs. (24) and (26), of the left eigenvector of the rate matrix. This agreement would not be achieved were we to choose, for example, $\Phi_{\{\mathbf{m}\}}(\mathbf{k})$ [Eq. (19)] to represent both $\Phi^{\mathrm{v}}_{\{\mathbf{m}\},\mathrm{prm}}(\mathbf{k})$ and $\Phi^{\mathrm{v}}_{\{\mathbf{m}'\},\mathrm{sec}}(\mathbf{k})$.

In real systems, however, no true discontinuity at $\theta=0.5$ is expected, except for $T=0$, because even for θ slightly above 0.5, for example, some holes in the F sublattice are present due to thermal fluctuations. They affect somewhat the atomic migration which is, however, controlled primarily by the kinetics of extra atoms in the E sublattice. What is expected, therefore, is a rapid variation of the diffusion coefficient over a relatively small coverage interval spanning $\theta=0.5$.

It is worthwhile at this point to compare our results with the results of an analytic approach by Chumak and Uebing[16] to diffusion in the interacting lattice gas on a square lattice for strongly repulsive interactions. They concentrate on coverages in the vicinity of $\theta=0.5$ at which the adsorbate forms the $c(2\times 2)$ structure, ignore the interactions of the activated particles (which corresponds to $J'=0$, i.e., $\sigma=1$), and base their approach on the factorization (1) of the diffusion coefficient considering the thermodynamics and the migration of defects separately. For the latter they consider the "white" and "black defects" corresponding roughly to one hole or atom, and the "white" and "black dimers," i.e., two holes or atoms close enough to the hopping atom to affect its hopping rate. White or black triads are not considered.

The entire philosophy of the approach in Ref. 16 is different from ours and it is rather difficult to make a comparison of their complete result with ours. Relative merits of both approaches can, however, be fully appreciated by comparing the results of Ref. 16 with ours for the case when the defect dimers are ignored. In this case, Eq. (34) in Ref. 16—transcribed into our notation—reads:

$$\begin{aligned} D(\theta) &= 2Wa^2\left[1+\frac{1}{\gamma}+\left(\frac{1}{\gamma}-1\right)\frac{\theta-0.5}{\sqrt{(\theta-0.5)^2+\gamma^4}}\right]\\ &\approx 2Wa^2\begin{cases}2, & \text{for } \theta<0.5\\ 2/\gamma, & \text{for } \theta>0.5,\end{cases}\end{aligned} \tag{38}$$

where the second line is obtained in the strong repulsion limit, $\gamma \ll 1$. Effectively, with defect dimers ignored, the diffusion coefficient does not depend in Ref. 16 on coverage except for the discontinuity at $\theta=0.5$ agreeing for $\sigma=1$ with that in Eq. (37). The weak dependence on θ on both sides of the discontinuity, formally present in the first line of Eq. (38) is due to the thermal fluctuations discussed in the paragraph following Eq. (37) and can be completely ignored for any coverage except when $|\theta-0.5| \leqslant \gamma^4 \ll 1$. According to Chumak and Uebing, defect dimers are necessary to get a genuine θ dependence of D on both sides of $\theta=0.5$. The result in Eq. (38) can be compared and contrasted with our results in Eqs. (34) and (36) in which we set $\sigma=1$ and ignore the second and the third terms in the square brackets (corresponding, respectively, to dimers and triads):

$$D(\theta) = 2Wa^2\begin{cases}8\theta^2, & \text{for } \theta<0.5\\ 8(1-\theta)^2/\gamma, & \text{for } \theta>0.5.\end{cases} \tag{39}$$

Here, the discontinuity is not smoothed out but a marked dependence on θ appears on both sides of it already when single defects (holes or extra atoms) are accounted for. This dependence is further modified by accounting for particle or hole dimers or triads.

IV. NUMERICAL RESULTS AND DISCUSSION

In Fig. 1 theoretical dependence $D(\theta)$ is plotted using Eqs. (34) and (36) for several values of the bridge site interaction parameters J' [cf. Eq. (3)] and compared with the results of the Monte Carlo simulations.[23] The adsorption site interaction parameter J is set at $10k_BT/3$ ($\gamma=0.036$). For $J=0$ (the topmost curve) the height of the potential barrier at the bridge site is unaffected by the interatomic interactions. Increasing J (i.e., lowering σ) raises the height of the potential barrier leading, as seen in Fig. 1, to less efficient diffusion. The data are shown only for the coverage interval $0.35 \leqslant \theta \leqslant 0.65$ within which the lattice gas is in a structurally staggered phase well below the critical temperature. At coverages near the limits of the interval our analytic approach is not valid because the system undergoes, according to the simulations, a structural phase transformation.

We see that the agreement between theory and simulations is good but there are deviations, most pronounced for $J'=0$ for high coverges ($\theta>0.5$) and for $J'=2J$ for low coverages ($\theta<0.5$). Theory overestimates the diffusion efficiency in both cases. The discrepancy can be traced back to the oversimplified treatment of the process shown in the diagram in Eq. (20f) between configurations A_3 and A_3^* for $n=+3$ (three close to each other extra atoms in the E sublattice) for $\theta>0.5$ and the analogous process for $\theta<0.5$ for $n=-3$

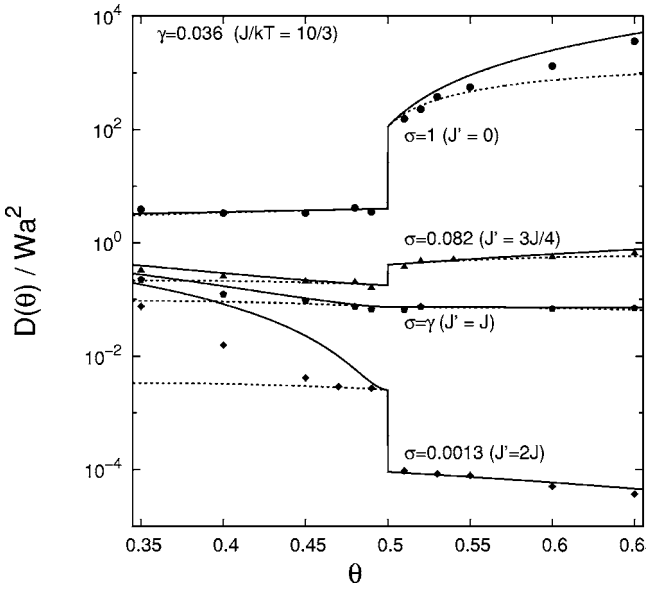

FIG. 1. Coverage dependence of the diffusion coefficient for several sets of interaction parameters. Solid line: theoretical results from Eqs. (34) and (36); dashed line : theoretical results without contributions proportional to $(1-2\theta)^2$ due to three extra atoms (for $\theta>0.5$) or holes (for $\theta<0.5$) in the active cell; and points: results of Monte Carlo simulations.

(three close to each other holes in the F sublattice). Before discussing this in detail in the following paragraph, we pause to consider the case $\theta>0.5$ and concentrate on the diagram in Eq. (20f) corresponding to $n=+3$. One may argue that transitions between the configurations A_3 and A_3^* should not contribute directly to a long range mass transport because the jumping atom is trapped in a cage formed by occupied sites surrounding it. A similar argument might apply to the transitions corresponding to $n=-3$ for $\theta<0.5$. The error due to this effect is expected to be the largest when $\sigma/\gamma \gg 1$ for θ well above 0.5 and when $\sigma \ll 1$ for θ well below 0.5 because for these parameters the contributions due to $n=+3$ and $n=-3$ diagrams to Eqs. (34) and (36) respectively, dominate. This is evident in Fig. 1: $J'=0$ corresponds to $\sigma/\gamma=28$ while $J'=2J$ corresponds to $\sigma=1/784$. Ignoring, *ad hoc*, the $n=\pm 3$ contributions in $D(\theta)$ leads to the results shown by dashes in Fig. 1—the agreement gets improved in the vicinity of $\theta=0.5$ but further away the efficiency of diffusion is underestimated this time.

Certainly [returning, to be specific, to $n=+3$ and the diagram in Eq. (20f)], transitions between configurations A_3 and A_3^* do influence diffusion. In contrast to $n=+1$ or $+2$ cases, however, local configurations A_3 and A_3^* are equally probable so designating A_3^* as a secondary one is not correct. Note that evaluating the environmental factor for an active cell with n extra atoms, we allow the $\delta N-n$ extra atoms within the environment to be distributed among the sites of the E sublattice only while keeping filled all sites of the F sublattice. In other words, counting configurations of the *environment*, we admit within it all local arrangements resembling primary configurations A_n but exclude the secondary ones A_n^* on a basis that they are much less probable. This is not correct, however, for local arrangements of the A_3^* type which, being as probable as A_3, should be accounted for when the configurations of the environment are counted—one should admit some F sites within the environment to be vacated by an atom transferred to a neighboring E site if three other E sites surrounding this pair of sites are also filled by extra atoms. Missing the local configurations of the A_3^* type from the environment factors in the numerator $\mathfrak{M}(\mathbf{k})$ is partially compensated by their simultaneous omission in the denominator $\mathfrak{N}(\mathbf{k})$, as already mentioned below Eq. (25).

Globally, local arrangements of the A_3^* type become important only when δN becomes a significant fraction of N, i.e., for coverages substantially higher than 0.5 because only then simultaneous filling of three neighboring E sites is likely. In effect, one expects that accounting correctly for the role played by the A_3^* configurations would result in the first two terms within the square bracket in Eq. (34) to be multiplied by coverage dependent factors equal to 1 for $\theta=0.5$ and deviating from it with increasing coverage. Such a correction would entirely replace the third term. The same arguments apply, of course, to the $\theta<0.5$ case modifying Eq. (36) in the same way. Unfortunately, the only possibility for fully consistent treatment of local arrangements with three neighboring extra atoms ($n=+3$) or holes ($n=-3$) seems to be repeating the entire calculations using active cells with many more sites than the four shown in Eq. (28). This has not been done yet because our recent investigations of diffusion in a one-dimensional interacting lattice gas[24] direct us to an approach to the evaluation of both $\mathfrak{M}(\mathbf{k})$ and $\mathfrak{N}(\mathbf{k})$ allowing one to treat a wider class of atom-atom interactions.

One of the features of our analytic result is that the diffusion coefficient in Eq. (36) for a rarefied gas ($\theta<0.5$) does not depend on γ, i.e., it is independent on the adsorption-site interatomic interaction energy J. Naively, one might expect that this implies that in the case of no bridge-site interatomic interactions, $J'=0, \sigma=1$, one should expect the coverage independent diffusion coefficient for $\theta<0.5$. This, of course, is not the case in Eq. (36) despite the fact that all relevant primary-to-secondary configuration transition rates, listed in Eq. (35), are, indeed, all the same in this case. The dependence on θ is due to the fact that the J interactions still matter: rates of the return jumps, from the secondary to the primary configurations, do depend on γ—they are at least $1/\gamma$ times faster than those in Eq. (35). γ does not appear in the final result for $D(\theta)$ only because $\gamma \ll 1$. To check this point we compare, in Figs. 2 and 3, our analytic results with the results of simulations for $\sigma=0.082$ and $\sigma=1$, respectively. In both cases the independence of $D(\theta)$ on J is confirmed by numerical simulations. In fact, agreement between theory and simulations for $\theta<0.5$ is in Fig. 2 better than expected in view of the fact that we have $\sigma \ll 1$ here. For $\theta>0.5$ the agreement is also reasonably good even if we have $\sigma/\gamma>1$ for all presented curves in both figures.

V. CONCLUSIONS

We have applied in this paper a recently designed[17] analytic approach to collective diffusion in an interacting lattice gas to a two-dimensional adsorbate ordered below the critical temperature by strongly repulsive interatomic interac-

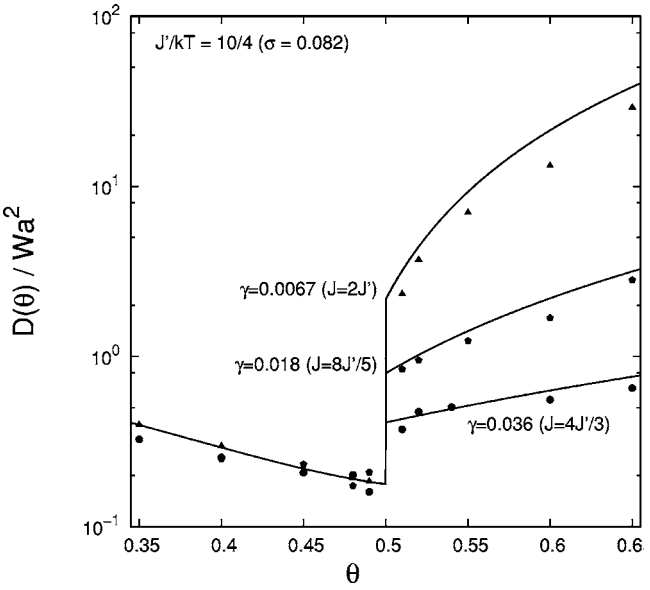

FIG. 2. Coverage dependence of the diffusion coefficient for several sets of interaction parameters J and $\sigma=0.082\ll 1$.

tions. We have allowed for interactions of a hopping atom with other atoms adsorbed at sites nearest to the site from which hopping occurs and nearest to the bridge site over which the atom jumps. An algebraic expression for a coverage dependent diffusion coefficient is extracted by evaluating a long wavelength limit of the diffusive eigenvalue of a master equation describing a random walk kinetics of *microscopic* states of the adsorbate. A variational approach is used in which plausible candidates for the left and right diffusive eigenvectors of the master equation rate matrix are proposed and then used to evaluate the eigenvalue. Equilibrium correlations, organization of the adsorbate into a structural $c(2\times 2)$ staggered phase are accounted for by appropriately designing the eigenvectors.

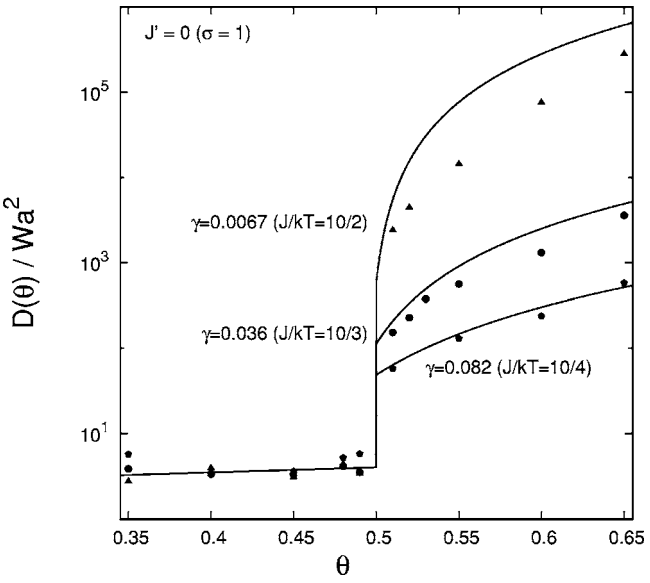

FIG. 3. Coverage dependence of the diffusion coefficient for several sets of adsorption-site interactions parameters J and $J'=0(\sigma=1)$ corresponding to no bridge-site interatomic interactions.

Analytic results for the coverage dependence of the chemical diffusion coefficient were compared with the results of Monte Carlo simulations of diffusion for the lattice gas with the same interatomic interactions. In general, the agreement is very good and a source of observed discrepancies is well understood. Improvements of the model are possible at a cost of more complicated and tedious combinatorics. Rather than following this path we intend to generalize the approach in the same manner as it was done recently for a one-dimensional lattice gas with arbitrary repulsive/attractive interactions.[20,24]

Advantages of our approach, as we see them, are (i) It is free of uncertainties usually associated with various truncation schemes of the hierarchy of equations for correlations. In our approach the diffusion coefficient is extracted directly from the microscopic kinetics of the system. (ii) The diffusion coefficient is not *a priori* factorized into the kinematic and the thermodynamic factors, which are usually treated independently of each other using often mutually incompatible approximation schemes. Even if it would be tempting to associate the numerator and the denominator [cf. Eqs. (14), (17), and (18)] with the kinematic and the static factors, respectively (which at this point we are not ready to do), both factors are evaluated in our approach using the same approximation schemes. (iii) By confronting results of our approach with the results of Monte Carlo simulations one is able to test which types of microscopic configurations of the system, affecting the kinetics of the random walk, are essential for the long range mass transport. This is so because proposing variational candidates for the eigenvectors one must either account for or ignore some classes of configurations. The variational anzatz made in this work takes advantage of the fact that for the low temperature structurally ordered phase one can classify the relevant mass transport microscopic configurations of the gas into the primary ones (having relatively large equilibrium probability) and the secondary (transient) ones. These two classes of configurations have to be treated differently.

A disadvantage of our approach, on the other hand, is analogous to that of the variational method in quantum mechanics: the result is only as accurate as allowed by the accuracy of the variational guess for the left (and right) eigenvector of the rate matrix. This point requires further investigation into the formal properties of such eigenvectors.

On a technical side, the combinatorics associated with our approach may become intimidatingly complicated because the number of particles in the system as well as its size must be kept fixed throughout the calculation. This difficulty might be overcome by opening the system and introducing a Lagrange multiplier akin to the chemical potential which would assure that the size of the system matches the actual one on average. A step in this direction was actually made in our investigation of collective diffusion in a one-dimensional interacting lattice gas,[20,24]

ACKNOWLEDGMENTS

This work was partially supported by research grants from NSERC (the Natural Science and Engineering Research

Council of Canada—Z.W.G.) and from KBN (Committee for Scientific Research of Poland, Grant No. 2 P03B 048 24—M.Z.K.).

APPENDIX A

We provide here considerations which justify the choice of $\Phi^{\nu}_{\{\mathbf{m}\},\mathrm{prm}}(\mathbf{k})$ and $\Phi^{\nu}_{\{\mathbf{m}\},\mathrm{sec}}(\mathbf{k})$ in Eqs. (24) and (26), respectively. To this end we consider a random walk of a single atom in one dimension along a periodic chain of adsorption sites. There are two types of sites: strongly binding type 1 site (represented by $\diamond$) followed along the chain by a weakly binding type 2 (represented by $\circ$)followed by type 1 again, etc., as shown in the diagram below

$$\ldots|\diamond\circ|\diamond\circ|\diamond\circ|\diamond\circ|\diamond\circ|\diamond\circ|\ldots. \tag{A1}$$

Vertical lines denote the boundaries of the lattice elementary cells and the lattice constant is a. We also assume that the height of the potential barrier separating a given site from a neighboring site to its right is different than that to its left—here it means that the barrier height within each cell is different from that for barriers at the cell boundaries. There are four jump rates: the rates out of the deeper $\diamond$ sites are denoted W_l and W_r, for the leftward and rightward jumps, respectively, and the rates out of the shallow $\circ$ sites are, respectively, V_l and V_r. The rates of jumps in the opposite directions between a given pair of sites are related to each other through the detailed balance condition

$$\frac{W_r}{V_l} = \frac{W_l}{V_r} = \alpha, \tag{A2}$$

where α is the ratio of the equilibrium occupation probability at the shallow $\circ$ site to that at the deep $\diamond$ site. We assume that $\alpha \ll 1$. If the atom is adsorbed at any deep $\diamond$ site then the system is in a primary configuration. Otherwise, it is in a secondary one.

It is now easy to write the rate equations for the nonequilibrium occupation probabilities of both sites in a lattice elementary cell ℓ. After taking the lattice Fourier transform [cf. Eq. (9)] one gets the set of two equations for $P_1(k,t)$ and $P_2(k,t)$ which can be written in the same form as Eq. (10) with the rate matrix being

$$\mathbb{M}(k) = \begin{pmatrix} -(W_l + W_r), & (W_r + W_l e^{ika})/\alpha \\ W_r + W_l e^{-ika}, & -(W_l + W_r)/\alpha \end{pmatrix}. \tag{A3}$$

We are interested in the diffusive eigenvalue $-\lambda(k)$ of this matrix and corresponding to it the left eigenvector $\tilde{\mathbf{e}}(k)$. This can be done exactly but for our purpose the expressions for $\alpha \ll 1$ are easier to interpret. The approximate expression for the eigenvalue is

$$-\lambda(k) \approx \frac{4W_l W_r}{W_l + W_r} \sin^2\left(\frac{ka}{2}\right), \tag{A4}$$

and the Hermitian conjugate of the corresponding left eigenvector is

$$\tilde{\mathbf{e}}^{\dagger}(k) \approx \begin{pmatrix} e^{-ik0} \\ \dfrac{W_r}{W_l + W_r} e^{-ik0} + \dfrac{W_l}{W_l + W_r} e^{-ika} \end{pmatrix}, \tag{A5}$$

where we have written explicitly $\exp(-ik0)$ instead of 1.

This form justifies the forms of the primary and secondary components of $\mathbf{\Phi}^{\nu}(\mathbf{k})$ proposed in Eqs. (24) and (26). The first component of $\tilde{e}^{\dagger}(k)$, corresponding to the primary configuration—the atom adsorbed at the deep $\diamond$ site in the $\ell = 0$ elementary cell—is equal to the phase factor $\exp(-ik0) = 1$ associated with this site. For a many-atom system a single phase factor is replaced with a sum of phase factors, i.e., with $\Phi_{\{\mathbf{m}\}}(\mathbf{k})$ defined in Eq. (19). This is the result proposed in Eq. (24) for the primary configuration components $\Phi^{\nu}_{\{\mathbf{m}\},\mathrm{prm}}(\mathbf{k})$.

The second component in Eq. (A5), corresponding to the secondary configuration—the atom adsorbed at the shallow $\circ$ site in the $\ell = 0$ cell–is equal to the average of the phase factors $\exp(-ik0)$ and $\exp(-ika)$, contributed by the neighboring deep $\diamond$ sites (i.e., neighboring primary configurations), weighted by the jump rates from these primary configurations to the secondary configuration under consideration. The $\diamond$ site to the left of the $\circ$ in question is in the same $\ell = 0$ cell as the $\circ$ and the jump rate from it is W_r, so its contribution is $\propto W_r \exp(-ik0)$. The $\diamond$ site to the right of the $\circ$ is in the $\ell = +1$ cell, the jump rate from this site is W_l, so its contribution is $\propto W_l \exp(-ika)$. This is exactly the structure of $\Phi_{\{\mathbf{m}\},\mathrm{sec}}(\mathbf{k})$ in Eq. (26) after the phase factors corresponding to the two primary configurations are replaced with their generalizations [Eq. (19)] appropriate for the many-atom system.

We can now clarify the statement made in the last sentence in the paragraph containing Eq. (26). Beside the diffusive eigenvalue $-\lambda(k)$ given in Eq. (A4) the rate matrix $\mathbb{M}(k)$, given in Eq. (A3), also has another eigenvalue, which does not vanish when $ka \to 0$ and is responsible for a transient time evolution that terminates well before the diffusion sets in. The result of these transients is to populate the secondary configuration, i.e., to populate the shallow adsorption sites $\circ$, even if they were not populated at $t = 0$. The second component of $\tilde{\mathbf{e}}^{\dagger}(k)$ sets the phase factors appropriate for these configurations.

APPENDIX B

We use here the diagrams in Eq. (20) to evaluate the factors $\mathcal{C}_{\alpha}(\mathbf{k})$ in Eq. (21) which are not, evaluated in the main text. For $\alpha = A_1'$ the considerations are similar to these leading to Eq. (30). The secondary configuration $A_1'^{*}$ can either be obtained from the primary configuration A_1' [as shown in Eq. (20c)] in which the extra atom is at (1, 0) and the hopping atom jumps from (0, 0) to (0, 1) to get $A_1'^{*}$, or from another primary configuration $\hat{A}_1'$ in which the extra atom is at the site (0, 1) and the hopping atom jumps from (0, 0) to (1, 0). The jump rate is W_1^3 in both cases so, according to Eqs. (22) and (26),

$$\Phi_{A_1',\mathrm{sec}} = \frac{1}{2}\left(\Phi_{A_1'} + \Phi_{\hat{A}_1'}\right),$$

$$\mathcal{C}_{A_1'}(\mathbf{k}) = \frac{1}{4}\left|\Phi_{A_1'}(\mathbf{k}) - \Phi_{\hat{A}_1'}(\mathbf{k})\right|^2 = \frac{1}{4}\left|f_{0,1} - f_{1,0}\right|^2. \quad \text{(B1)}$$

This accounts for the arrangement shown in Eq. (20c) where the primary jump is from left to right. The leftward primary jump is accounted for by adding a contribution in which $f_{0,1}$ is replaced with $f_{0,\bar{1}}$ and similar contributions must be added for two possible primary jump directions for each of the remaining three possible placements of the extra atom within the cell. The sum of all eight $\mathcal{C}_\alpha$'s in this case, which in Eq. (21) are multiplied by the primary jump rate W_1^3 and the environmental factor $\mathfrak{D}(4,1;L^2/2,\delta N)$, is

$$\mathcal{C}_1'(\mathbf{k}) = \frac{1}{2}\left(\left|f_{0,1} - f_{1,0}\right|^2 + \left|f_{0,\bar{1}} - f_{1,0}\right|^2 + \left|f_{0,1} - f_{\bar{1},0}\right|^2 + \left|f_{0,\bar{1}} - f_{\bar{1},0}\right|^2\right) = 4\left[\sin^2\left(\frac{a}{2}(k_x + k_y)\right) + \sin^2\left(\frac{a}{2}(k_x - k_y)\right)\right] \to 2(ka)^2. \quad \text{(B2)}$$

For $\alpha = A_2$, Eq. (20d), a new element appears because the secondary configuration A_2^* can be reached from three primary ones. Besides A_2 from which the transition rate is W_2^4, we have $\hat{A}_2$ in which the extra atoms occupy the sites (0,1) and $(\bar{1},0)$ and the hopping atom jumps from (0, 0) to (1, 0) to get A_2^*, and $\tilde{A}_2$ with the extra atoms at (1, 0) at (1,0) and the hopping atom jumps to $(\bar{1},0)$. The transition rate from either one of these two primary configurations to A_2^* is W_2^3. From Eqs. (22) and (26) we get

$$\Phi_{A_2,\mathrm{sec}} = \frac{1}{2+\sigma}(\sigma\Phi_{A_2} + \Phi_{\hat{A}_2} + \Phi_{\tilde{A}_2}),$$

$$\mathcal{C}_{A_2}(\mathbf{k}) = \frac{1}{(2+\sigma)^2}\left|2\Phi_{A_2} - \Phi_{\hat{A}_2} - \Phi_{\tilde{A}_2}\right|^2 = \frac{1}{(2+\sigma)^2}\left|f_{1,0} + f_{\bar{1},0} - 2f_{0,1}\right|^2, \quad \text{(B3)}$$

where σ is defined in Eq. (3). This accounts only for the rightward primary jump shown in Eq. (20d). Contributions due to the leftward primary jump and two primary jump directions for the horizontal placement of the two extra atoms must be added, resulting in

$$\mathcal{C}_2(\mathbf{k}) = \frac{1}{(2+\sigma)^2}\left(\left|f_{1,0} + f_{\bar{1},0} - 2f_{0,1}\right|^2 + \left|f_{1,0} + f_{\bar{1},0} - 2f_{0,\bar{1}}\right|^2 + \left|f_{0,1} + f_{0,\bar{1}} - 2f_{1,0}\right|^2 + \left|f_{0,1} + f_{0,\bar{1}} - 2f_{\bar{1},0}\right|^2\right) = \frac{8}{(2+\sigma)^2}\left[4\sin^2\left(\frac{a}{2}(k_x + k_y)\right) + 4\sin^2\left(\frac{a}{2}(k_x - k_y)\right) - \sin^2(k_x a) - \sin^2(k_y a)\right] \to \frac{8}{(2+\sigma)^2}(ka)^2, \quad \text{(B4)}$$

which must be multiplied by the primary jump rate W_2^4 and $\mathfrak{D}(4,2;L^2/2,\delta N)$ to account for four $n=2$ contributions to Eq. (21).

For $\alpha = A_2'$ the procedure is the same. The primary configurations from which transitions to the secondary $A_2'^*$ are possible are A_2' and similar to it $\hat{A}_2'$ in which the two extra atoms are (1, 0) and (0, 1) [the hopping atom jumps from (0, 0) to $(0,\bar{1})$ in the latter]. The jump rate from each of them is W_2^3. The third possible primary configuration is $\tilde{A}_2'$ with the extra atoms at (0, 1) and $(0,\bar{1})$ and the hopping atom jumping to (1, 0) at the rate W_2^4. We get

$$\Phi_{A_2',\mathrm{sec}} = \frac{1}{2+\sigma}\left[\sigma\Phi_{\tilde{A}_2'} + \Phi_{A_2'} + \Phi_{\hat{A}_2'}\right],$$

$$\mathcal{C}_{A_2'}(\mathbf{k}) = \frac{1}{(2+\sigma)^2}\left|(1+\sigma)\Phi_{A_2'} - \Phi_{\hat{A}_2'} - \sigma\Phi_{\tilde{A}_2'}\right|^2 = \frac{1}{(2+\sigma)^2}\left|(f_{0,\bar{1}} - f_{0,1}) + \sigma(f_{1,0} - f_{0,1})\right|^2. \quad \text{(B5)}$$

Accounting for four possible ways the two extra atoms can be placed around the hopping atom and for two directions of the primary jump for each case requires adding eight terms of this type. The result, which in Eq. (21) gets multiplied by the primary jump rate W_2^3 and the environmental factor $\mathfrak{D}(4,2;L^2/2,\delta N)$, is

$$\mathcal{C}_2'(\mathbf{k}) = \frac{2}{(2+\sigma)^2}\left(\left|(f_{0,\bar{1}} - f_{0,1}) + \sigma(f_{1,0} - f_{0,1})\right|^2 + \left|(f_{1,0} - f_{\bar{1},0}) + \sigma(f_{0,\bar{1}} - f_{\bar{1},0})\right|^2 + \left|(f_{0,1} - f_{0,\bar{1}}) + \sigma(f_{1,0} - f_{0,\bar{1}})\right|^2 + \left|(f_{1,0} - f_{\bar{1},0}) + \sigma(f_{0,1} - f_{\bar{1},0})\right|^2\right) = \frac{16}{(2+\sigma)^2}\left\{(1+\sigma)\left[\sin^2(k_x a) + \sin^2(k_y a)\right] + \sigma^2\left[\sin^2\left(\frac{a}{2}(k_x + k_y)\right) + \sin^2\left(\frac{a}{2}(k_x - k_y)\right)\right]\right\} \to \frac{8}{(2+\sigma)^2}(\sigma^2 + 2\sigma + 2)(ka)^2. \quad \text{(B6)}$$

The case $\alpha = A_3$ is somewhat different because the A_3^* configuration is as probable as A_3. Consequently, we should use Eq. (24) rather than Eq. (26) to get $\Phi_{A_3,\mathrm{sec}}$. Therefore

$$\mathcal{C}_{A_3}(\mathbf{k}) = \left|\Phi_{A_3}(\mathbf{k}) - \Phi_{A_3^*}(\mathbf{k})\right|^2 = \left|f_{0,0} - f_{0,1}\right|^2. \quad \text{(B7)}$$

Adding three similar contributions for the remaining primary jump directions we get

$$\mathcal{C}_3(\mathbf{k}) = \left|f_{0,0} - f_{0,1}\right|^2 + \left|f_{0,0} - f_{\bar{1},0}\right|^2 + \left|f_{0,0} - f_{0,\bar{1}}\right|^2 + \left|f_{0,0} - f_{1,0}\right|^2 = 8\left[\sin^2\left(\frac{k_x a}{2}\right) + \sin^2\left(\frac{k_y a}{2}\right)\right] \to 2(ka)^2, \quad \text{(B8)}$$

which, after being multiplied by the primary jump rate W_3^4 and the environmental factor $\mathfrak{D}(4,3;L^2/2,\delta N)$ accounts for four $n=3$ contributions to Eq. (21).

*Electronic address: zalum@ifpan.edu.pl
†Electronic address: gortel@phys.ualberta.ca

[1] R. Gomer, Rep. Prog. Phys. **53**, 917 (1990).
[2] V. P. Zhdanov, *Elementary Physicochemical Processes on Solid Surfaces* (Plenum, New York, 1991).
[3] A. Danani, R. Ferrando, E. Scalas, and M. Torri, Int. J. Mod. Phys. B **11**, 2217 (1997).
[4] T. Ala-Nissila, R. Ferrando, and S. C. Ying, Adv. Phys. **51**, 949 (2002).
[5] H. J. Kreuzer, in *Diffusion at Interfaces: Microscopic Concepts*, Vol. 12 of Springer Series in Surface Science, edited by M. Grunze, H. J. Kreuzer, and J. J. Weimar (Springer, New York, 1988), p. 63.
[6] H. J. Kreuzer and J. Zhang, Appl. Phys. A: Solids Surf. **51**, 183 (1990).
[7] H. J. Kreuzer, J. Chem. Soc., Faraday Trans. **86**, 1299 (1990).
[8] J. A. Venables, G. D. Spiller, and M. Hanbrücken, Rep. Prog. Phys. **47**, 399 (1984).
[9] A. Pimpinelli and J. Villain, *Physics of Crystal Growth* (Cambridge University Press, Cambridge, England 1998).
[10] P. Jensen, Rev. Mod. Phys. **71**, 1695 (1999).
[11] J. V. Barth, Surf. Sci. Rep. **40**, 75 (2000).
[12] T. T. Tsong, Surf. Sci. **64**, 199 (2000); Prog. Surf. Sci. **67**, 235 (2001).
[13] M. Giesen, Surf. Sci. **68**, 1 (2001).
[14] A. V. Myshlyavtsev, A. A. Stepanov, C. Uebing, and V. P. Zhdanov, Phys. Rev. B **52**, 5977 (1995).
[15] D. A. Reed and G. Ehrlich, Surf. Sci. **102**, 588 (1981).
[16] A. A. Chumak and C. Uebing, Eur. Phys. J. B **9**, 323 (1999).
[17] Z. W. Gortel and M. A. Załuska-Kotur, Phys. Rev. B **70**, 125431 (2004).
[18] A. Sadiq and K. Binder, Surf. Sci. **128**, 350 (1983).
[19] H. J. Kreuzer and Z. W. Gortel, *Physisorption Kinetics*, Vol. 1 of Springer Series in Surface Science (Springer, New York, 1986), Chap. 1.
[20] Ł. Badowski, M. A. Zaluska-Kotur, and Z. W. Gortel, Phys. Rev. B **72**, 245413 (2005).
[21] In the sets $\{\mathbf{m}\}$ and $\{\mathbf{m}'\}$ in Eq. (22) we have $\mathbf{m}_i=\mathbf{m}'_i$ for all atoms i except for the one which executes the jump by $\mathbf{a}$. For the latter $\mathbf{m}_i$ and $\mathbf{m}'_i$ differ by $\mathbf{a}/|\mathbf{a}|$. If the configurations $\{\mathbf{m}\}$ and $\{\mathbf{m}'\}$ were related to each other by a jump of the reference atom then all $\mathbf{m}_i$'s would differ by $\mathbf{a}/|\mathbf{a}|$ from the corresponding $\mathbf{m}'_i$'s and then a phase factor $\exp(i\mathbf{k}\cdot\mathbf{a})$ would multiply one of the terms within the absolute value sign in Eq. (22). The key point is that the resulting absolute value does not depend on what the label of the hopping atom is—it depends only on its local environment, labeled by α. For details see Ref. 17.
[22] M. A. Załuska-Kotur, Z. W. Gortel, and R. Teshima, Phys. Rev. B **66**, 165418 (2002).
[23] Monte Carlo simulations were performed as described in M. A. Załuska-Kotur, S. Krukowski, and Ł. A. Turski, Surf. Sci. **441**, 320 (1999); M. A. Załuska-Kotur, S. Krukowski, Z. Romanowski, and Ł. A. Turski, *ibid.* **457**, 357 (2000).
[24] M. A. Załuska-Kotur, Ł. Badowski, and Z. W. Gortel, Physica A **357**, 305 (2005). In this approach the sums over configurations in $\mathfrak{M}(\mathbf{k})$ and $\mathfrak{N}(\mathbf{k})$ are opened in the same spirit as it is done in standard statistical mechanics when the canonical ensemble approach is replaced with the grand canonical one. One injects into the system extra holes/atoms and lattice sites effectively removing intractable restrictions in the sums over configuration. This requires introducing an extra parameter, analog of fugacity, whose value is fixed by the actual atom density.